Materials Today Chemistry 26 (2022) 101171

Contents lists available at ScienceDirect

Materials Today Chemistry

journal homepage: www.journals.elsevier.com/materials-today-chemistry/

UV light blocking and conversion by porous europium-doped titanium dioxide (TiO_2-Eu) thin films for potential protection of photovoltaic devices

K. Zhumanova [a], L. Serik [a], A. Molkenova [a, b], T.S. Atabaev [a, *]

[a] Department of Chemistry, Nazarbayev University, Nur-Sultan, 010000, Kazakhstan
[b] Institute of Advanced Organic Materials, Pusan National University, Busan, 46241, South Korea

ARTICLE INFO

Article history:
Received 3 July 2022
Received in revised form
17 August 2022
Accepted 23 August 2022
Available online 23 September 2022

Keywords:
Coatings
UV protection
Europium-doped TiO_2
Downconversion
Spectral converter

ABSTRACT

In recent years, transparent thin films capable of screening and converting ultraviolet (UV) photons into visible spectrum gained significant interest in the protection of photovoltaic devices. We investigated the optical properties and UV screening capability of europium-doped titanium oxide (TiO_2—Eu) thin films deposited by the spin-coating method from a solution precursor for the first time in this study. We showed that TiO_2-Eu thin films demonstrate europium concentration-dependent optical properties, and the quantum yield of the optimized sample was found to be ~10.2%. Transmittance and photoluminescence measurements suggested that TiO_2—Eu thin film can effectively block UV photons (~30.5% at 320 nm) at glass substrate and convert them to the red emission thanks to $^5D_0 \rightarrow {}^7F_j$ (j = 0, 1, 2, 3, and 4) Eu (III) electronic transitions. Photodegradation experiments with methylene blue dye revealed that TiO_2—Eu thin films offer better UV protection compared to uncoated samples. We strongly believe that porous TiO_2—Eu thin films can be effectively utilized as a UV blocking and light conversion coating.

1. Introduction

In recent years, thin films with excellent fluorescent/luminescent properties gained substantial interest from the scientific community. In particular, thin films with fluorescent/luminescent properties can be employed in a range of applications, such as remote temperature sensing [1,2], solid-state lighting [3,4], improving solar cells efficiency [5,6], security labeling [7], white LED fabrication [8], and so on. Despite the remarkable progress in thin-film fabrication, conventional methods such as pulsed laser deposition, sputtering, atomic layer deposition, and chemical vapor deposition are resource- and time-consuming, hence, hardly applicable for mass production [1–9]. The sol-gel method can be considered as a low-cost process; however, it is also not suitable for some applications because of poor control over film thickness and surface topography [9,10]. In this regard, the development of new methods for the deposition of luminescent films is appealing from both a scientific and technological perspective.

The presence of organic components in the third-generation photovoltaic devices such as dye-synthesized, organic, and perovskite solar cells make them vulnerable to photodegradation under direct sunlight exposure. Several research groups proposed interface modification, the introduction of various additives, and the use of ultraviolet (UV)-filters to address photodegradation issues [11–14]. The deposition of transparent UV-filters based on wide bandgap TiO_2, ZnO, and WO_3 materials is considered to be a promising approach due to their abundance and inexpensive cost. For example, a composite layer of TiO_2 and WO_3 can improve UV-blocking properties leading to a better stability of perovskite solar cells [14]. Johansson et al. showed that TiO_2 and ZnO coatings can also significantly reduce the transmittance of destructive UV photons [15]. On the other hand, partial blocking of UV photons can diminish the efficiency of solar cells [14]. In this scenario, the above-mentioned problem can be solved by the introduction of UV-to-visible converting optical materials into the UV-blocking thin films [16,17]. To date, the synthesis of UV-to-visible converting optical materials and their simultaneous deposition with UV-blocking thin films appears to be a challenging task. Several issues can be outlined here such as (a) controlling the deposition of UV-blocking film and the insertion of optical nanomaterials at the

* Corresponding author.
E-mail address: timur.atabaev@nu.edu.kz (T.S. Atabaev).

https://doi.org/10.1016/j.mtchem.2022.101171

same time, (b) a problem with the homogeneous distribution of optical nanomaterials in thin films, (c) issues with even film deposition due to the presence of nanostructures, (d) potential luminescence quenching of optical materials in UV-blocking films, and so on. To tackle this issue, our research group has recently proposed a facile deposition method of transparent and luminescent titanium oxide-based thin films with dual functionality [7]. Here, titanium oxide-based thin films doped with a fixed concentration of europium (Eu) were tested as a potential security marker and UV blocking film [7]. However, it is well known that the luminescent properties of lanthanide-based optical materials are strongly dependent on the optical activator concentration and should be optimized to avoid quenching of luminescence caused by cross-relaxation effects [18,19]. To the best of our knowledge, a simple solution-based coating method and concentration-dependent study have never been reported before, making this study fairly unique. A new experimental procedure for testing the UV-protective properties of thin films using light-sensitive methylene blue dye solution was also introduced. Overall, it was found that concentration-optimized Eu-doped titanium oxide thin films can reduce the destructive UV photon transmittance and effectively convert them into visible light photons.

2. Materials and methods

2.1. Deposition procedure

Anhydrous isopropanol (99.5%), 1-butanol (99.9%), titanium (IV) isopropoxide (≥ 97%), and europium nitrate pentahydrate ($Eu(NO_3)_3 \times 5H_2O$, 99.9%) were procured from Merck & Co. Precursor solution synthesis was carried out using a slightly modified version of our earlier protocol [7]. In brief, a certain amount of $Eu(NO_3)_3 \times 5H_2O$ was dissolved in 0.5 mL of isopropanol and then mixed with 1 mL of 1-butanol and 100 μL of titanium (IV) isopropoxide. Glass substrates were thoroughly cleaned with ethanol and deionized water prior to deposition. A spin-coating method (3000 rpm, 15 s) was used to deposit thin layers on the glass slides. Coated films were allowed to dry in air for 2 h before being annealed at 500 °C for 1 h (ramping rate of 5 °C/min).

2.2. Characterization of Eu-doped TiO_2 thin films

The morphology, surface texture, and roughness of formed films were studied using atomic force microscopy (AFM, SmartSPM 1000) and scanning electron microscopy (SEM Crossbeam 540). Energy dispersive X-ray spectroscopy (EDX, Aztec, Oxford Instruments) was used to determine the elemental composition of the thin films. The X-ray diffraction (SmartLab X-ray Diffractometer, Rigaku Corp.) was utilized to analyze the structural properties of thin films. The chemical surface analysis of obtained films was examined using X-ray photoelectron spectroscopy (XPS, Nexsa G2, Thermo Fisher Scientific Inc.). A Genesys 50 UV–Vis spectrophotometer (Thermo Fisher Scientific Inc.) was used for absorbance/transmittance measurements. Photoluminescence (PL) analysis of TiO_2-Eu thin films was performed using an absolute quantum yield spectrometer (C11347-11, Hamamatsu Photonics K.K.). All measurements were repeated three times at room temperature conditions.

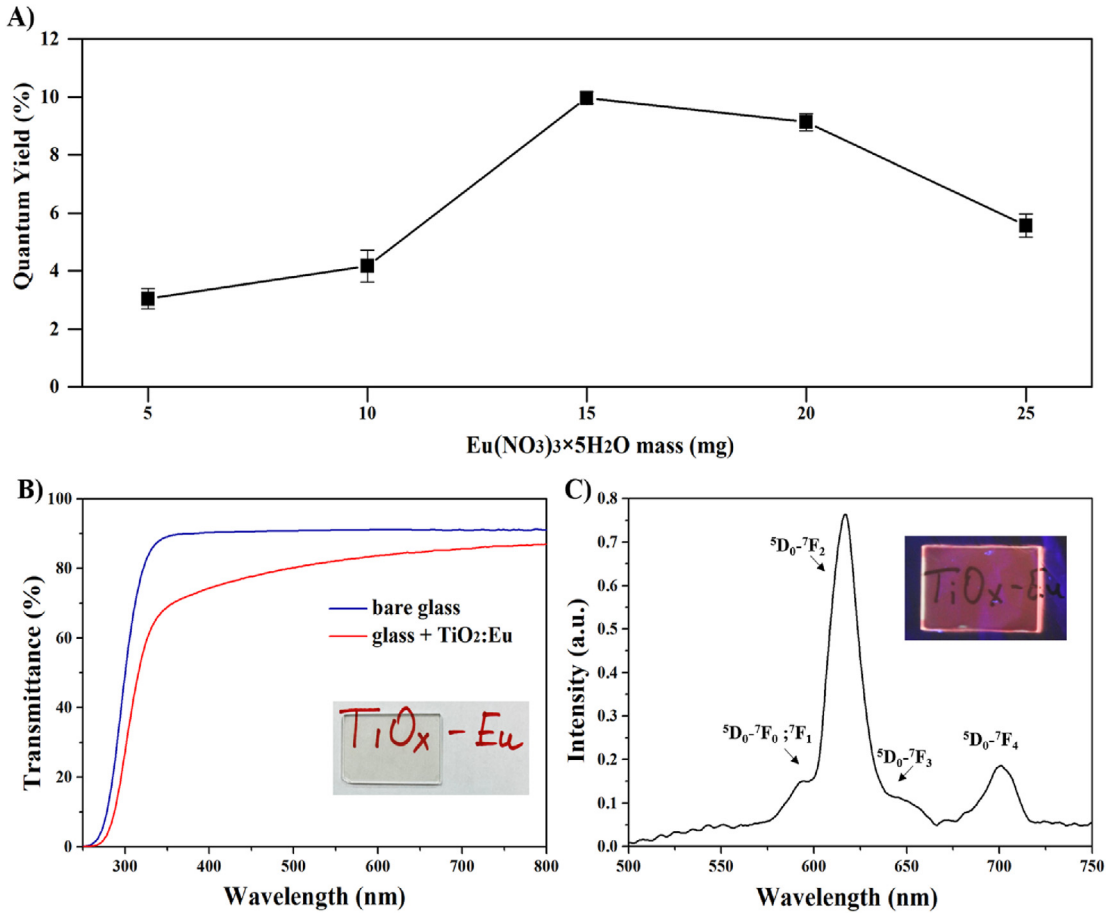

Fig. 1. **(a)** Quantum yield dependence on the salt concentration. **(b)** Transmittance spectra of TiO_2-Eu thin film. **(c)** Photoluminescence spectra of TiO_2-Eu thin film.

3. Results and discussion

Table ST1 (Supporting Information) summarizes recent advances in the fabrication of TiO_2-based films for UV protection. As one can see, the solution-based deposition of luminescent TiO_2 films has never been done before, highlighting the novelty of the current study. A PL spectrometer was used to determine the optimal europium doping concentration in TiO_2 thin films. Fig. 1A depicts the quantum yield (QY) dependence on the mass of europium salt added to precursor solutions. As can be seen, films with 15 mg of $Eu(NO_3)_3 \times 5H_2O$ achieve the highest QY (~10.2%), which then decreases due to cross-relaxation quenching [18,19]. The same sample also exhibited higher luminescent and better UV-blocking properties, as shown in Figs. S1 and S2 (Supporting Information). Figs. 1B and C show the light transmission and emission characteristics of the film with the highest QY, i.e. optimized sample. The prepared film is optically transparent (Fig. 1B), ensuring photon transmission in the visible-IR range [20]. However, detailed analysis revealed that all TiO_2-Eu films significantly reduces the transmittance of destructive UV photons. In particular, the UV photons' transmittance at 320 nm and 365 nm for optimized sample (Fig. 1B) was decreased to 30.5% and 20.9%, respectively. It is also worth mentioning that there are no significant differences in the transmittance of films deposited at different speeds, i.e. the transmittance of films deposited at 2000, 3000, and 4000 rpm was reduced to 29.9, 30.5, and 29.4% at 320 nm, respectively. From one side, UV blocking can protect UV-sensitive devices and ensure their long-term operational stability. On the other hand, a partial loss of photons reaching the active layer of solar harnessing systems can reduce their effectiveness. Hence, conversion of UV photons into visible photons can partially compensate loss of UV photons, because emitted visible photons can be absorbed by active materials in some photovoltaic devices. Fig. 1C shows the PL emission spectra of the optimized TiO_2-Eu thin film ($\lambda_{exc} = 310$ nm). Four characteristic Eu emission peaks centered at 594 nm ($^5D_0 \rightarrow {}^7F_0$;$^7F_1$), 617 nm ($^5D_0 \rightarrow {}^7F_2$), 651 nm ($^5D_0 \rightarrow {}^7F_3$), and 701 nm ($^5D_0 \rightarrow {}^7F_4$) were detected in the PL emission spectra [21]. The intensity of the $^5D_0$-$^7F_2$ transition at 617 nm clearly dominates; thus, the luminescence of TiO_2-Eu thin film appears red to the naked eye (Fig. 1C inset). The Tauc method was used to evaluate the optical bandgap of the optimized TiO_2-Eu thin film [22]. The optical bandgap of the optimized film was found to be ~3.37 eV (Fig. S3, Supporting Information), while the optical bandgap of anatase TiO_2 is known to be ~3.21 eV [15]. The difference in optical bandgap values between TiO_2-Eu and TiO_2 can be explained by the presence of Eu dopant, as the bandgap of bare Eu_2O_3 was reported to be 4.3 eV [23].

AFM and SEM were further used to examine the surface morphology and thickness of the optimal TiO_2-Eu thin film. Both AFM and SEM measurements (Fig. 2A–F, and S4 (Supporting Information)) revealed that the TiO_2-Eu thin films has a porous structure (pore size ~45 ± 12 nm), which is most likely the result of NO_x gas release during the thermal treatment. Indeed, AFM analysis of an undoped TiO_2 film and doped TiO_2-Eu films (Fig. 2) confirms our hypothesis, as the density of pores increases with the amount of europium salt for films with 15, 20, and 25 mg of salt, respectively. The thickness of the prepared TiO_2-Eu thin films deposited at 3000 rpm was in the range of ~32–35 nm, as shown in Fig. S4 (Supporting Information). According to several studies, porous structures can serve as effective light-trapping and anti-reflective coatings [24,25]. Hence, it is anticipated that porous TiO_2-Eu thin film with UV blocking/conversion ability can be a promising candidate for the potential protection of UV-sensitive components in third generation solar cells.

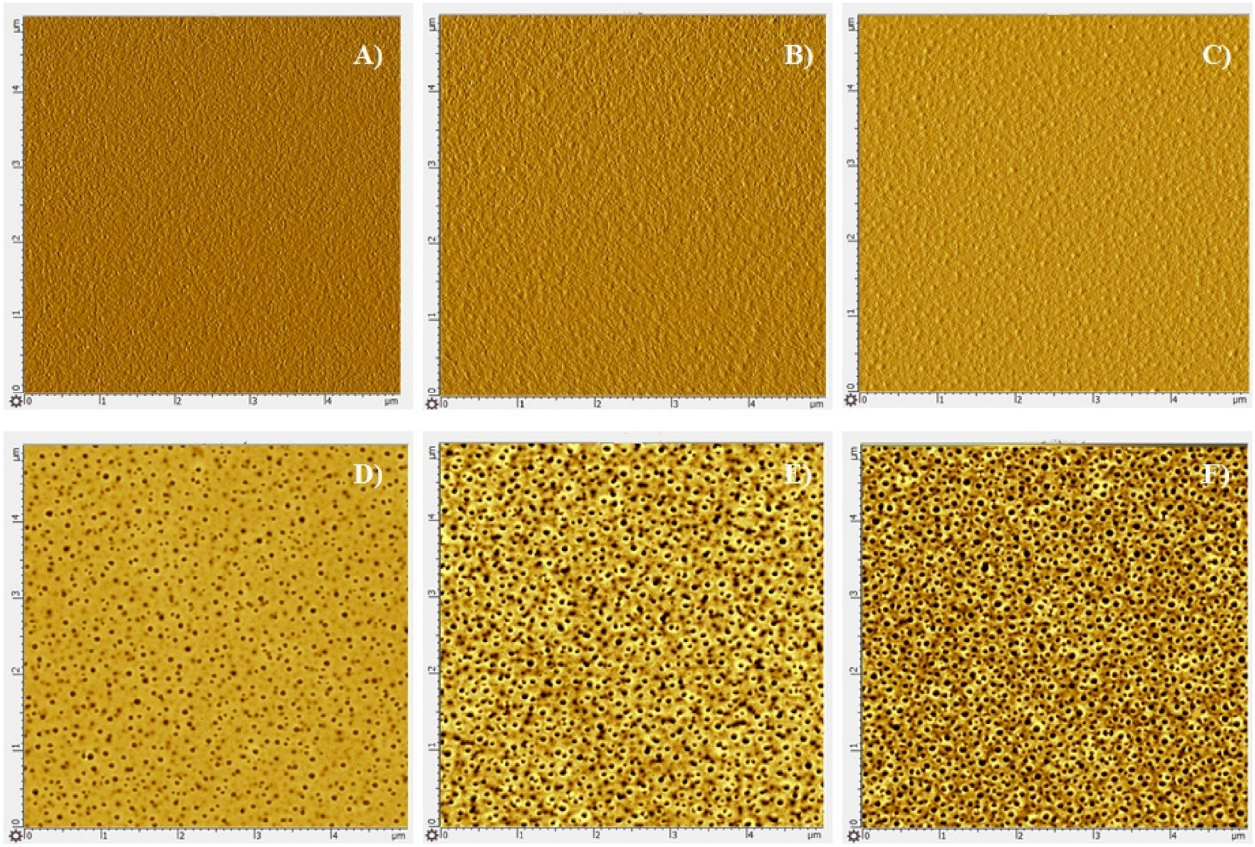

Fig. 2. AFM analysis of **(a)** bare TiO_2, **(b)** TiO_2-Eu (5), **(c)** TiO_2-Eu (10), **(d)** TiO_2-Eu (15), **(e)** TiO_2-Eu (20), and **(f)** TiO_2-Eu (25) films. AFM, atomic force microscopy.

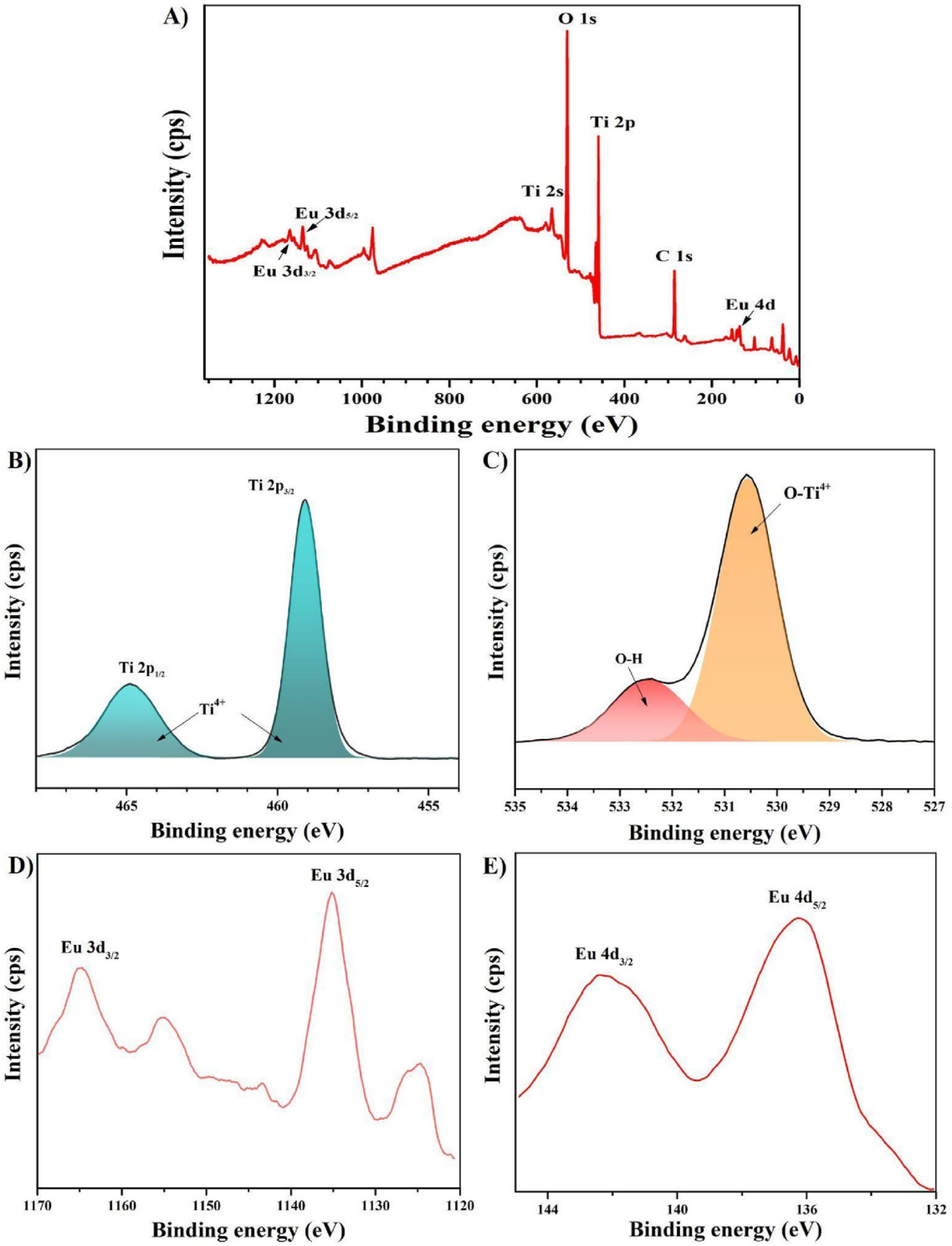

Fig. 3. (**a**) XPS full scan survey spectra of TiO_2-Eu thin films. XPS spectra of (**b**) Ti 2p, (**c**) O 1s, (**d**) Eu 3d, and (**e**) Eu 4d regions. XPS, X-ray photoelectron spectroscopy.

Surface and elemental analysis of the optimized film were further tested using XPS and EDX. EDX elemental mapping (Fig. S5, Supporting Information) confirmed that Ti, O, and Eu elements are uniformly distributed in a selected area. The full XPS survey scan of TiO_2-Eu thin film is shown in Fig. 3A. The survey spectra reveal the presence of titanium, oxygen, europium, and carbon on the surface of the film. The presence of a carbon peak at 284.9 eV is usually attributed to the surface contamination [26]. Fig. 3B shows a high-resolution Ti 2p spectrum with two peaks at 459.1 eV (Ti $2p_{3/2}$) and 464.8 eV (Ti $2p_{1/2}$), indicating that Ti has the highest (Ti^{4+}) oxidation state [27]. The narrow scan spectra of O1s (Fig. 3C) revealed that the main peak at 530.6 eV is associated with oxygen atoms bonded to (Ti^{4+}), whereas the peak at 532.5 eV is attributed to the hydroxyl (−OH) groups or adsorbed water molecules [28]. Fig. 3D shows the 1135.1 eV (Eu $3d_{5/2}$) and 1164.8 eV (Eu $3d_{3/2}$) spin-orbit split peaks in the Eu3d core-level spectrum. Furthermore, two

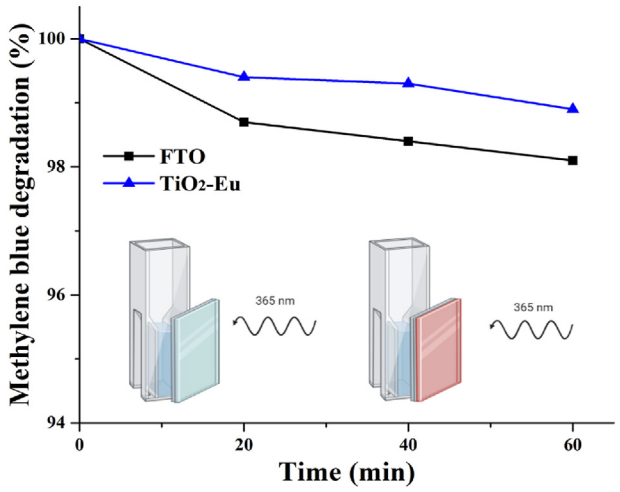

Fig. 4. Degradation kinetics of MB dye with uncoated/coated FTO substrates. FTO, fluoride tin oxide; MB, methylene blue.

peaks were detected at 136.6 eV (Eu $4d_{5/2}$) and 142.4 eV (Eu $4d_{3/2}$) corresponding to the Eu^{3+} oxidation state, which is well consistent with the PL emission spectrum [29].

A light sensitive aqueous solution of methylene blue (MB) dye (1×10^{-5} M) was used to assess the UV blocking properties of TiO_2—Eu thin films. Protective coating was applied to fluorine-doped tin oxide (FTO) glass substrate (commonly used substrate in photovoltaics) and then placed in front of quartz cuvettes with MB solution. A bare FTO glass substrate was used as a control. A commercial UV lamp ($\lambda = 365$ nm, 8 W) was placed 5 cm away from the samples at dark room conditions and has been used as a source of UVA radiation. The degradation of the MB dye was monitored every 20 min at 664 nm using a UV—Vis spectrophotometer. Fig. 4 clearly shows that the degradation of MB is effectively reduced with coated FTO glass substrate as compared to uncoated one. In particular, it was found that the film-protected MB dye degraded to 42.1% less in 1 h than that of the control sample. These indirect measurements clearly show that TiO_2—Eu coating can provide adequate protection to UV-sensitive components. Furthermore, the porous structure and UV to visible light conversion properties of TiO_2—Eu coating make it a good candidate for use with third generation photovoltaic devices such as perovskite and dye-sensitized solar cells.

4. Conclusions

In conclusion, a simple and straightforward solution-based strategy for the deposition of porous TiO_2-Eu films with UV-blocking and downconversion properties was proposed. It was revealed that the optimized sample can effectively block UV radiation (~30.5% at 320 nm) and convert UV to visible light with a QY of ~10.2%. MB degradation experiments successfully confirmed the UV-blocking properties of TiO_2—Eu coating. We strongly believe that a proposed methodology can be implemented for the protection of photovoltaic devices and for the development of new UV-blocking coatings.

Credit author statement

Kamila Zhumanova: Formal analysis, Investigation, Writing — original draft, **Lazzat Serik:** Formal analysis, Investigation, Writing — original draft, **Anara Molkenova:** Methodology, Validation, Data curation, Writing — original draft, **Timur Sh. Atabaev**: Methodology, Validation, Resources, Supervision, Writing — review and editing.

Funding

This research was funded by Nazarbayev University FDCRDG, Grant No. 240919FD3929.

Declaration of competing interest

The authors declare that they have no known competing financial interests or personal relationships that could have appeared to influence the work reported in this paper.

Data availability

Data will be made available on request.

Appendix A. Supplementary data

Supplementary data to this article can be found online at https://doi.org/10.1016/j.mtchem.2022.101171.

References

[1] M.N. Getz, O. Nilsen, P.-A. Hansen, Sensors for optical thermometry based on luminescence from layered YVO_4: Ln^{3+} (Ln = Nd, Sm, Eu, Dy, Ho, Er, Tm, Yb) thin films made by atomic layer deposition, Sci. Rep. 9 (2019), 10247, https://doi.org/10.1038/s41598-019-46694-8.
[2] K.M. Schreiter, T. Glawdel, J.A. Forrest, C.L. Ren, Robust thin-film fluorescence thermometry for prolonged measurements in microfluidic devices, RSC Adv. 3 (2013), 17236, https://doi.org/10.1039/c3ra41368c.
[3] J. Prakash, V. Kumar, L.J.B. Erasmus, M.M. Duvenhage, G. Sathiyan, S. Bellucci, S. Sun, H.C. Swart, Phosphor polymer nanocomposite: ZnO:Tb^{3+} embedded polystyrene nanocomposite thin films for solid-state lighting applications, ACS Appl. Nano Mater. 1 (2018) 977—988, https://doi.org/10.1021/acsanm.7b00387.
[4] S. Cho, Properties of Eu-doped YVO_4 thin films grown on glass substrates by radio-frequency magnetron sputtering, Appl. Phys. A 127 (2021) 161, https://doi.org/10.1007/s00339-021-04308-z.
[5] W.-L. Jeong, J. Jang, J. Kim, S.-K. Joo, M.-D. Park, H.-M. Kwak, J. Baik, H.-J. Kim, J.H. Kim, D.-S. Lee, Improving ultraviolet responses in $Cu_2ZnSn(S,Se)_4$ thin-film solar cells using quantum dot-based luminescent down-shifting layer, Nanomaterials 11 (2021) 1166, https://doi.org/10.3390/nano11051166.
[6] A. Ghazy, M. Safdar, M. Lastusaari, A. Aho, A. Tukiainen, H. Savin, M. Guina, M. Karppinen, Luminescent $(Er,Ho)_2O_3$ thin films by ALD to enhance the performance of silicon solar cells, Sol. Energy Mater. Sol. Cell. 219 (2021), 110787, https://doi.org/10.1016/j.solmat.2020.110787.
[7] A. Molkenova, L. Khamkhash, A. Zhussupbekova, K. Zhussupbekov, S. Sarsenov, I. Taniguchi, I.V. Shvets, T.Sh Atabaev, Solution-based deposition of transparent Eu-doped titanium oxide thin films for potential security labeling and UV screening, Nanomaterials 10 (2020) 1132, https://doi.org/10.3390/nano10061132.
[8] S. Bindai, K. Annapurna, A. Tarafder, Realization of phosphor-in-glass thin film on soda-lime silicate glass with low sintering temperature for high color rendering white LEDs, Appl. Opt. 58 (2019) 2372, https://doi.org/10.1364/AO.58.002372.
[9] Y. Zhang, J. Hao, Metal-ion doped luminescent thin films for optoelectronic applications, J. Mater. Chem. C 1 (2013) 5607, https://doi.org/10.1039/c3tc31024h.
[10] L. Benharrat, L. Guerbous, D. Bradai, A. Boukerika, A. Manseri, N. Selmi, B. Rahal, M.S.E. Hamroun, Preparation and characterization of luminescent YPO_4: Eu^{3+} thin films using sol gel spin coating method, Thin Solid Films 694 (2020), 137738, https://doi.org/10.1016/j.tsf.2019.137738.
[11] Y. Wu, H. Zhu, B.-B. Yu, S. Akin, Y. Liu, Z. Shen, L. Pan, H. Cai, Interface modification to achieve high-efficiency and stable perovskite solar cells, Chem. Eng. J. 433 (2022), 134613, https://doi.org/10.1016/j.cej.2022.134613.
[12] Z. Wang, Z. Zhang, L. Xie, S. Wang, C. Yang, C. Fang, F. Hao, Recent advances and perspectives of photostability for halide perovskite solar cells, Adv. Opt. Mater. 10 (2022), 2101822, https://doi.org/10.1002/adom.202101822.
[13] A. Mahapatra, S. Kumar, P. Kumar, B. Pradhan, Recent progress in perovskite solar cells: challenges from efficiency to stability, Mater. Today Chem. 23 (2022), 100686, https://doi.org/10.1016/j.mtchem.2021.100686.
[14] G. Aljaiuossi, Y.F. Makableh, M. Al-Fandi, Design and optimization of nano-structured UV-filters for efficient and stable perovskite solar cells, Semicond. Sci. Technol. 34 (2019), 125014, https://doi.org/10.1088/1361-6641/ab51a0.
[15] W. Johansson, A. Peralta, B. Jonson, S. Anand, L. Österlund, S. Karlsson, Transparent TiO_2 and ZnO thin films on glass for UV protection of PV modules, Front. Mater. 6 (2019) 259, https://doi.org/10.3389/fmats.2019.00259.
[16] M.B. de la Mora, O. Amelines-Sarria, B.M. Monroy, C.D. Hernández-Pérez, J.E. Lugo, Materials for downconversion in solar cells: perspectives and

challenges, Sol. Energy Mater. Sol. Cell. 165 (2017) 59–71, https://doi.org/10.1016/j.solmat.2017.02.016.
[17] X. Liu, T. Chen, Y. Gong, C. Li, L. Niu, S. Xu, X. Xu, L. Pan, J.G. Shapter, Y. Yamauchi, J. Na, M. Eguchi, Light-conversion phosphor nanoarchitectonics for improved light harvesting in sensitized solar cells, J. Photochem. Photobiol. C Photochem. Rev. 47 (2021), 100404, https://doi.org/10.1016/j.jphotochemrev.2021.100404.
[18] T.S. Atabaev, J.H. Lee, Y.C. Shin, D.-W. Han, K.S. Choo, U.B. Jeon, J.Y. Hwang, J.A. Yeom, H.-K. Kim, Y.-H. Hwang, Eu, Gd-codoped yttria nanoprobes for optical and T_1-weighted magnetic resonance imaging, Nanomaterials 7 (2017), 35, https://doi.org/10.3390/nano7020035.
[19] G. Lakshminarayana, E.M. Weis, A.C. Lira, U. Caldiño, D.J. Williams, M.P. Hehlen, Cross Relaxation in rare-earth-doped oxyfluoride glasses, J. Lumin. 139 (2013) 132–142, https://doi.org/10.1016/j.jlumin.2013.02.039.
[20] S. Khasym, A. Pasha, M. Lakshmi, P. Chellasamy, M. Kadarkarai, A.A.A. Darwish, T.A. Hamdalla, S.A. Al-Ghamdi, S. Alfadhli, Post treated PEDOT-PSS films with excellent conductivity and optical properties as multifunctional flexible electrodes for possible optoelectronic and energy storage applications, Opt. Mater. 125 (2022), 112109, https://doi.org/10.1016/j.optmat.2022.112109.
[21] W. Wang, P. Zhu, Red photoluminescent Eu^{3+}-doped Y_2O_3 nanospheres for LED-phosphor applications: synthesis and characterization, Opt Express 26 (2018), 34820, https://doi.org/10.1364/OE.26.034820.
[22] P. Makuła, M. Pacia, W. Macyk, How to correctly determine the band gap energy of modified semiconductor photocatalysts based on UV–Vis spectra, J. Phys. Chem. Lett. 9 (2018) 6814–6817, https://doi.org/10.1021/acs.jpclett.8b02892.
[23] T. Hadamek, S. Rangan, J. Viereck, D. Shin, A.B. Posadas, R.A. Bartynski, A.A. Demkov, Stoichiometry, band alignment, and electronic structure of Eu_2O_3 thin films studied by direct and inverse photoemission: a reevaluation of the electronic band structure, J. Appl. Phys. 127 (2020), 074101, https://doi.org/10.1063/1.5139227.
[24] A.S. Rad, A. Afshar, M. Azadeh, Anti-reflection and self-cleaning meso-porous TiO_2 coatings as solar systems protective layer: Investigation of effect of porosity and roughness, Opt. Mater. 107 (2020), 110027, https://doi.org/10.1016/j.optmat.2020.110027.
[25] T. Pickering, K. Shanks, S. Sundaram, Modelling technique and analysis of porous anti-reflective coatings for reducing wide angle reflectance of thin-film solar cells, J. Opt. 23 (2021), 025901, https://doi.org/10.1088/2040-8986/abeaec.
[26] D. Xue, J. Luo, Z. Li, Y. Yin, J. Shen, Enhanced photoelectrochemical properties from Mo-doped TiO_2 nanotube arrays film, Coatings 10 (2020) 75, https://doi.org/10.3390/coatings10010075.
[27] D. Kim, K.M. Kim, H. Han, J. Lee, D. Ko, K.R. Park, K. Jang, D. Kim, J.S. Forrester, S.H. Lee, J.C. Kim, S. Mhin, Ti/TiO_2/SiO_2 multilayer thin films with enhanced spectral selectivity for optical narrow bandpass filters, Sci. Rep. 12 (2022) 32, https://doi.org/10.1038/s41598-021-03935-z.
[28] B. Bharti, S. Kumar, H.-N. Lee, R. Kumar, Formation of oxygen vacancies and Ti^{3+} state in TiO_2 thin film and enhanced optical properties by air plasma treatment, Sci. Rep. 6 (2016), 32355, https://doi.org/10.1038/srep32355.
[29] D. Kim, Y.-H. Jin, K.-W. Jeon, S. Kim, S.-J. Kim, O.H. Han, D.-K. Seo, J.-C. Park, Blue-silica by Eu^{2+}-activator occupied in interstitial sites, RSC Adv. 5 (2015) 74790–74801, https://doi.org/10.1039/C5RA15641F.